MAGNETIC ANOMALIES IN LUNAR IMPACT BASINS: IMPLICATIONS FOR IMPACTOR TRAJECTORIES. L. L. Hood[1], J. S. Oliveira[2,3], J. Andrews-Hanna[1], M. A. Wieczorek[4], and S. Stewart[5], [1]Lunar and Planetary Laboratory, University of Arizona, Tucson, AZ 85721, USA, lon@lpl.arizona.edu, [2]ESA/ESTEC, SCI-S, Noordwijk, Netherlands, [3]CITEUC, Geophysical and Astronomical Observatory, University of Coimbra, Coimbra, Portugal, [4]Université Côte d'Azur, Observatoire de la Côte d'Azur, CNRS, Laboratoire Lagrange, Nice, France, [5]Dept. of Earth and Planetary Sciences, University of California, Davis.

Introduction: We report new mapping and interpretation of magnetic anomalies within three Nectarian aged lunar basins: Crisium, Mendel-Rydberg, and Moscoviense. These anomalies are likely to have sources consisting of impact melt enriched in metallic iron from the impactors that created the basins [1,2]. Comparisons of the new maps are made with previous numerical simulations of the impact of iron-rich planetesimals [1] to assess the likely trajectories of the impactors that created the basins. Inversions of the anomalies to estimate paleomagnetic pole positions are described in a related abstract by J. Oliveira et al.

Mapping Methods: While valuable global maps of the lunar crustal magnetic field have been constructed by several groups [e.g., 3,4], maps of improved accuracy and resolution over the three basins considered here can be constructed by selecting only the best orbital magnetometer measurements (lowest altitude and least amount of external field contamination) over these particular basins. Further improvements are obtained through careful editing and high-pass filtering of the selected measurements from either Lunar Prospector or Kaguya to minimize any remaining short- and long-wavelength external field contributions to the final maps. We consider only the observed radial field component, which is least affected by short-wavelength external fields, and apply a classical equivalent source dipole (ESD) technique [e.g., 5] to map the vector field components and field magnitude on a constant altitude surface. The ESD model dipoles are oriented radially inward or outward and are spaced at intervals of 2/3 degrees in latitude and longitude. The depth of the dipole array and all model dipole moments are chosen to minimize the RMS deviation of the model radial field component from the observed radial field component at the spacecraft altitude. Once the dipole moments and their orientations are determined, the vector field can be calculated on any constant altitude surface. However, the altitude should not be too far below the measurement altitudes to avoid downward continuation errors.

Mapping Results: Figure 1 shows maps of the field magnitude at 25 km altitude over the three basins superposed on LOLA topography. The contour interval is 1 nT starting at 2 nT. The depth of the dipole ar-

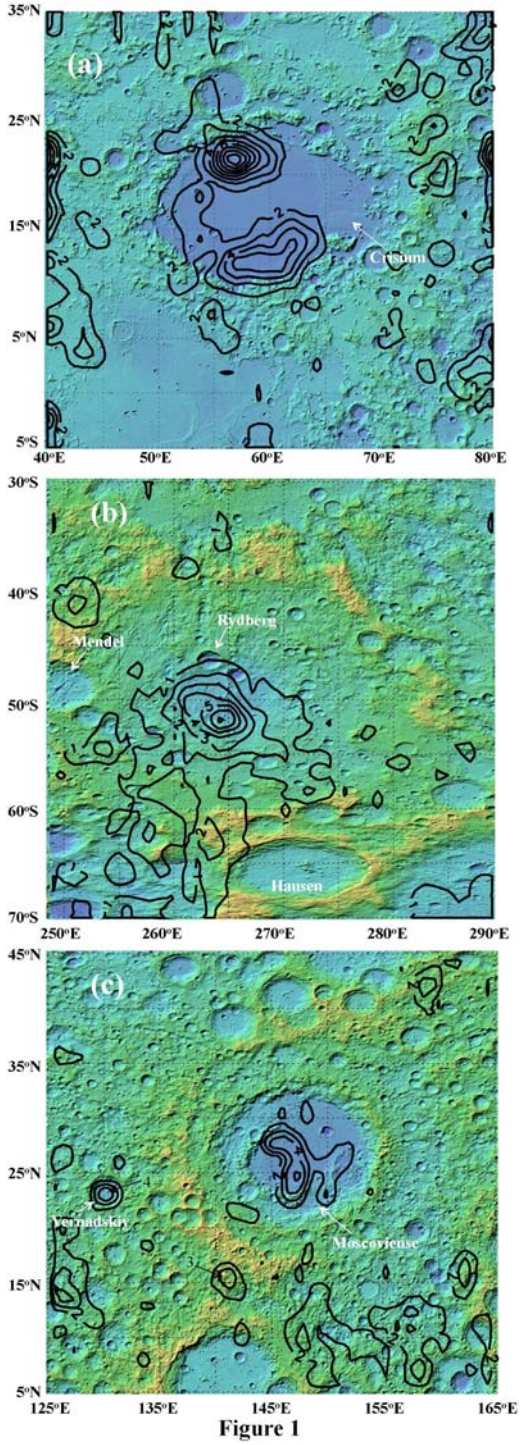

Figure 1

ray (determined by repeating the analysis at 5 km intervals and calculating the RMS deviation) was 10 km for all three basins. The model field was smoothed two-dimensionally to a resolution of ~ 1.2 degrees. The peak field intensities at this altitude within Crisium, Mendel-Rydberg, and Moscoviense are 9.5, 7, and 5 nT, respectively.

Impact Simulation Results: Wieczorek et al. [1] have reported modeling of the formation of a large lunar basin (SPA) via the impact of iron-rich planetesimals using a CTH shock physics code in three dimensions with self-gravity. For example, they investigated the impact of a 100 km radius differentiated impactor with a 55 km radius iron core impacting at 15 km/s. Although smaller basins should give similar results, the details may be slightly different. Briefly, it was found that for impact angles within ~ 50^o of vertical, most of the impactor iron was mixed into impact melt that was retained within the basin. For moderately oblique impacts (e.g., 30^o to 45^o from vertical), most of the iron-enriched melt was deposited on the downrange side of the basin interior. For very oblique impacts (e.g., 60^o from vertical), nearly all of the iron was mixed into ejecta that was deposited outside of the basin in the downrange direction.

Trajectory Implications: In the following, we first assume that the magnetic anomaly sources consist of iron-enriched impact melt beneath the visible mare basalt surface within the basin interiors. We then compare the implied iron distribution to the numerical simulations summarized above to infer probable trajectories of the impactors that created the basins. We note that all three basins have prominent central Bouguer gravity anomalies. However, the gravity anomalies are likely a consequence of mantle uplift following the impact and therefore do not provide direct information on the distribution of impactor iron.

Crisium: As shown in Figure 1a, the two strongest anomalies are located on the northern and southern sides of the basin interior. But the new mapping shows that these anomalies are connected by a band of weaker anomalies on the western side of the basin. If the sources are iron-enriched impact melt, the trajectory of the impactor that would be most consistent with the impact simulations is east-northeast to west-southwest at an angle of less than 60^o from vertical. This differs from previous suggestions of a west to east trajectory [e.g., 6], which were based partly on the interpretation of the elongated extension on the east side of the basin as being a result of a west to east oblique impact. However, an alternate interpretation of the eastward extension is that it represents a second smaller basin ("Crisium East") [7,8; see Fig. S10 of ref. 8]. The trajectory inferred here would support the latter interpretation.

Mendel-Rydberg: As shown in Figure 1b, the anomalies in this basin are concentrated on the southwestern side of the basin interior. The inferred impactor trajectory is therefore from northeast to southwest at an angle from the vertical of less than 60^o.

Moscoviense: Previous work suggests that this basin (with main ring diameter of 421 km centered at 26^oN, 147^oE) is the result of an impact onto a pre-existing larger basin [8,9]. The pre-existing basin (referred to as "Moscoviense North") has a main ring diameter of 640 km offset about 80 km to the northwest of Moscoviense itself. An inner 192-km diameter partial peak ring is nearly concentric with the 421-km diameter outer ring of the basin (see Fig. S16 of ref. 8).

As seen in Figure 1c, the main Moscoviense magnetic anomaly is centered on the east-northeast side of the inner peak ring and follows approximately the curvature of the ring. It is consistent with an oblique impact along a trajectory from west-southwest to east-northeast. No magnetic signature in the interior of the pre-existing Moscoviense North basin would remain because the later Moscoviense impact would have thermally erased it.

New mapping of magnetic anomalies in other lunar basins is underway.

Acknowledgments: Supported under a grant (80NSSC18K1602) from the NASA Lunar Data Analysis Program. The Lunar Prospector magnetometer data used here are available from the Planetary Plasma Interactions node of the NASA Planetary Data System at UCLA. The Kaguya magnetometer data are available from the Japan Aerospace Exploration Agency at: http://jlpeda.jaxa.jp/globalSVM20150511.zip.

References: [1] Wieczorek M. A. et al. (2012) *Science, 335,* 1212–1215. [2] Hood L. L. et al. (2018) *JGR Planets, 123,* 2647-2666. [3] Purucker, M. E. & J. B. Nicholas (2010), *JGR, 115,* E12007, doi:10.1029/2010JE003650. [4] Tsunakawa, H. et al. (2015), *JGR Planets, 120,* 1160-1185. [5] Hood L. L. (2016), *JGR Planets, 121,* 1016-1025. [6] Schultz P. H. & A. M. Stickle (2011) *LPS XLII,* Abstract 2611. [7] Frey H. V. (2011) In *Recent Advances and Current Research Issues in Lunar Stratigraphy*, W. A. Ambrose & D. A. Williams, Eds. (Spec. Paper 477, Geol. Soc. of America), pp. 53-75. [8] Neumann G. A. et al. (2015) *Sci. Adv., 1, No. 9,* e1500852. [9] Ishihara, Y. et al. (2011) *GRL, 38,* doi:10.1029/2010GL045887.